^{51}V NMR and magnetic susceptibility study of the strong-coupling superconductor HfV_2

Y. Kishimoto,[1] T. Ohno,[1] T. Hihara,[2] K. Sumiyama,[2] and K. Suzuki[2]
[1]*Department of Physics, Faculty of Engineering, Tokushima University, Tokushima 770-8506, Japan*
[2]*Institute for Materials Research, Tohoku University, Sendai 980-8577, Japan*
(Received 13 September 2000; revised manuscript received 19 December 2000; published 18 June 2001)

The Knight shift K of ^{51}V and the magnetic susceptibility χ in the $C15$ Laves phase compound HfV_2 have been measured to investigate the change in the electronic state at the martensitic lattice transformation temperature T_L and the symmetry of the superconducting order parameter. In the normal state, the hyperfine fields have been estimated to be -250 and $-72\,\mathrm{kOe}/\mu_B$ above and below T_L, respectively. The reduction in the magnitude of hyperfine field is considered to be due to a strong *s-d* mixing induced by the lattice transformation. Above T_L the V $3d$ derived density of states $N_{3d}(\varepsilon_F)$ obtained from K and the spin-lattice relaxation rate $1/T_1T$ is comparable with that estimated by a band calculation. The Knight shift due to $3d$ spin vanishes well below the superconducting transition temperature T_c. Since the T^5 dependence of $1/T_1$ well below T_c is explained by the anisotropic energy gap that has nodes at points on the Fermi surface, the Cooper pair is thought to be of Anderson-Brinkman-Morel $d\gamma$ or $d\varepsilon$ wave, for example.

DOI: 10.1103/PhysRevB.64.024509 PACS number(s): 74.70.Ad, 76.60.Cq, 76.60.Es

I. INTRODUCTION

The similarities in the physical properties between the conventional strong electron-phonon coupling superconductors, such as $A15$ and $C15$ Laves phase compounds, and the heavy Fermion superconductors (HFS) have been discussed.[1,2] Kusunose and Miyake[3] showed that the low-energy effective Hamiltonian of such a strongly coupled local electron-phonon system was mapped to the two-channel Kondo model. The logarithmic temperature dependence of the spin susceptibility observed in an $A15$ compound V_3Si could be explained by their theory.

One of the characteristics of $A15$ compounds V_3Si, Nb_3Sn and a $C15$ Laves phase compound HfV_2 is the saturation in the resistivity at high temperatures, where the mean free path of the conduction electrons is comparable to the lattice constant. Anderson and Yu[2] found that the conduction electrons in such a strong electron-phonon coupling system provide a double-well potential for the lattice ions. The ionic system in such a potential is called a two-level system (TLS). It was proved that a TLS plays a role of a localized $\frac{1}{2}$ spin in the Kondo system.[4] The periodic TLS corresponds to the dense Kondo system. Therefore, V_3Si, Nb_3Sn and HfV_2 are expected to show properties similar to those of the dense Kondo system. Since the temperature dependence of the electrical resistivity of HfV_2 (Ref. 5) is more unusual than that of $A15$ compounds, the investigation of the electronic state of HfV_2 is a subject of great interest.

One of the most important features of the HFS is the anisotropic energy gap formed by the strong correlation among conduction electrons composed of *f* and *s* electrons. As for the anisotropy of the superconducting energy gap of HfV_2, we have reported the results of spin-lattice relaxation rate $1/T_1$ of ^{51}V and specific-heat measurement.[6] $1/T_1$ exhibits a small coherence peak just below $T_c(=9.2\,\mathrm{K})$ and a T^5 dependence well below T_c. The specific heat obeys the T^3 law below T_c. We discussed these results in the frame of Anderson-Brinkman-Morel (ABM) model[7,8] in which the energy gap vanishes at the poles on the Fermi surface.

In the normal state $1/T_1T$ and χ of HfV_2, V_3Si and Nb_3Sn show a strong temperature dependence. This behavior can be attributed to a narrow conduction band with the bandwidth of about 100 K.[6,9–11] A peak in $1/T_1T$ was observed at about 110 K in HfV_2, where the martensitic lattice transformation is reported.[12] To investigate the change in the electronic states due to the martensitic transition and the symmetry of the superconducting order parameter in HfV_2, we have measured the Knight shift K of ^{51}V and the magnetic susceptibility χ. In Sec. II we describe the experimental procedure. In Sec. III we summarize the experimental results. In Sec. IV, we analyze the temperature dependence of χ, K, and $1/T_1T$ in the normal state consistently and estimate the density of electronic states. Finally, we discuss the symmetry of Cooper pair in the superconducting state in Sec. V, and give conclusion in Sec. VI.

II. EXPERIMENT

The sample is the same as used in Ref. 6. A polycrystalline sample was prepared from starting materials, Hf of 98% purity and V of 99.9% purity, by Ar plasma-jet melting. The ingot was turned over, melted ten times to ensure the homogeneity, and annealed at 1000 °C in a vacuum for a week. The obtained sample was crushed into the 200-mesh powder for the nuclear magnetic resonance (NMR) measurement. T_c was determined to be 9.2 K by the ac susceptibility and the electrical resistivity measurements. χ was measured with the superconducting quantum interference device magnetometer at IMR, Tohoku University. The ^{51}V NMR measurement was made with a conventional phase-coherent pulse spectrometer at 12 and 6 MHz.

III. EXPERIMENTAL RESULTS

The magnetization M measured at 10 and 290 K is plotted against the field H (M-H curves) in Fig. 1. The slope of each M-H curve is constant in the field range between 10 and 20

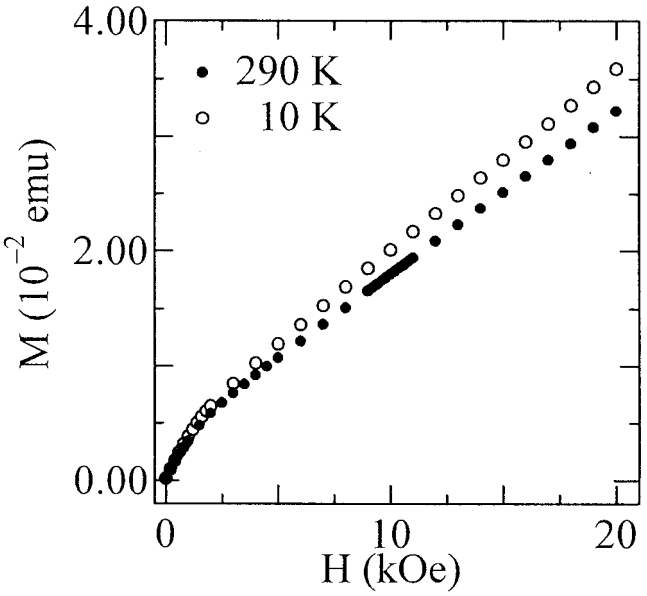

FIG. 1. Magnetization M vs applied magnetic field H curves measured at 10 (○) and 290 K (●).

kOe. Its anomaly observed in the low-field range indicates that M consists of an intrinsic paramagnetic part and a ferromagnetic impurity part as $M=\chi H+M_{\rm imp}(H)$. An example of the decomposition of M observed at 10 K is shown in Fig. 2. $M_{\rm imp}(H)$ saturates easily below 10 kOe. $M_{\rm imp}(H)$ estimated at 10 K agrees completely with that at 290 K. This implies that $M_{\rm imp}(H)$ is the same at any temperature between 10 and 290 K, and that the Curie temperature of the ferromagnetic impurity is much higher than 290 K. We think Fe

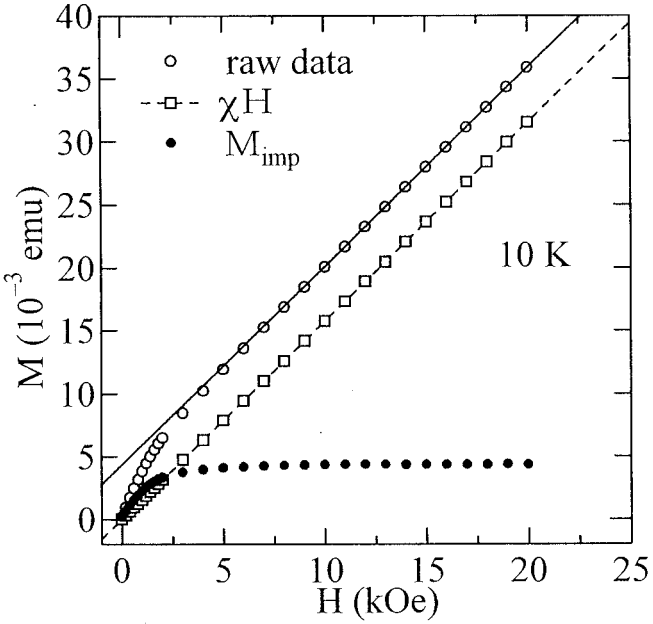

FIG. 2. M (open circles) observed at 10 K is decomposed into H-linear part $M=\chi H$ (dotted line and open squares) and impurity part $M_{\rm imp}(H)$ (closed circles).

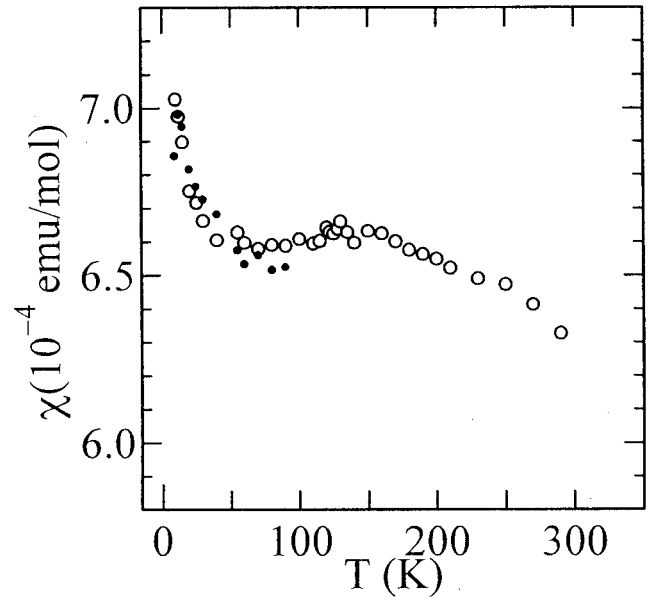

FIG. 3. Temperature dependence of magnetic susceptibility. χ calculated from the observed Knight shift K and Eq. (14) is shown by closed circles.

is contained as an impurity in the starting metals. Actually, Hf metal of purity 98% contains 415 ppm Fe according to an analysis table given by the supplier.[13] The V metal of purity 99.9% also contains 100 ppm Fe. From the value of the saturated $M_{\rm imp}(H)$, 3.76×10^{-3} emu, we find the content of Fe spins in HfV_2 to be 136 ppm, which is comparable with that estimated from the above reference values. We can es-

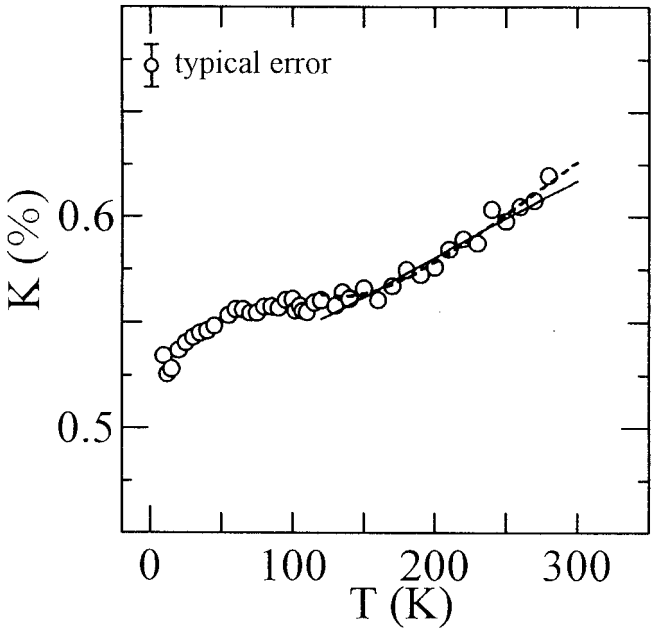

FIG. 4. Temperature dependence of ^{51}V Knight shift K in the normal state. Best fitting curves based on a *simple Lorentzian model* and a *two-peak model* are shown by solid and dotted curves, respectively.

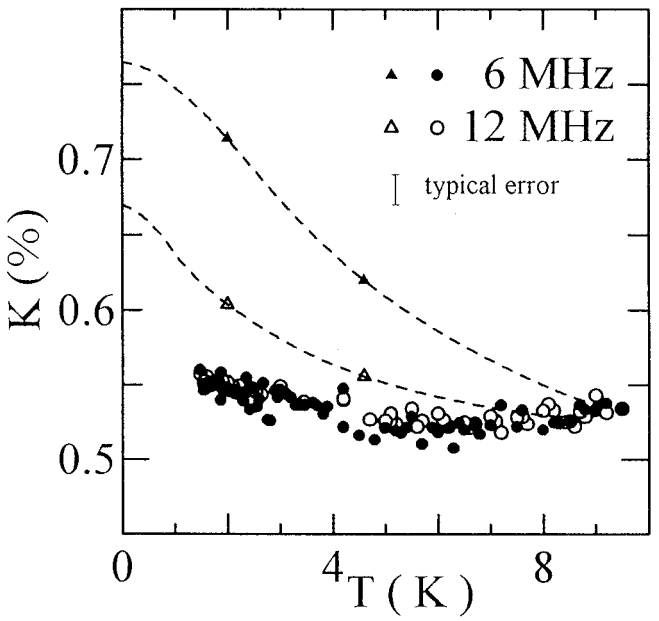

FIG. 5. Temperature dependence of K in the superconducting state measured at 12 (○) and 6 MHz (●). Corrected K at 4.6 and 2.0 K for the data observed at 12 (△) and 6 MHz (▲) are also shown. The broken curves illustrate the expected temperature dependence of the corrected K.

timate χ from the linear part of the magnetization, the temperature dependence of which is shown in Fig. 3. χ reported by Hafstrom, Knapp, and Aldred[14] is similar to ours above 60 K, but nearly constant below 60 K.

The NMR spectrum of ^{51}V consists of a narrow central peak and wide wing broadened by a distribution of the electric field gradient.[6]

The Knight shift K was estimated from the peak position of the spectrum. Figure 4 shows the temperature dependence of K in the normal state. The decrease in K with decreasing temperature is ascribed to the increase in the core-polarization due to V $3d$ spin associated with the increase in χ. The temperature dependence of K in the superconducting state is shown in Fig. 5. The difference between K measured at 12 MHz and that at 6 MHz is very small. K decreases slightly with decreasing temperature and then increases below 6 K. K in the superconducting state contains a large diamagnetic shift $K_{\rm dia}$ due to the Meissner effect. To estimate the intrinsic K, we measured the magnetization M in the superconducting state. Figure 6 shows the field dependence of M at 4.6 and 2.0 K.

Figure 7 shows the temperature dependence of $1/T_1T$ of ^{51}V reported in the previous paper.[6] $1/T_1T$ is nearly constant ($=0.12\ {\rm s}^{-1}{\rm K}^{-1}$) below 20 K.

IV. ANALYSIS OF THE TEMPERATURE DEPENDENCE OF χ, K, AND $1/T_1T$ IN THE NORMAL STATE

A. K-χ plot

The increase in χ between 290 and 120 K with decreasing temperature suggests the existence of a narrow d band. The decrease in χ below 120 K is attributed to the change in the

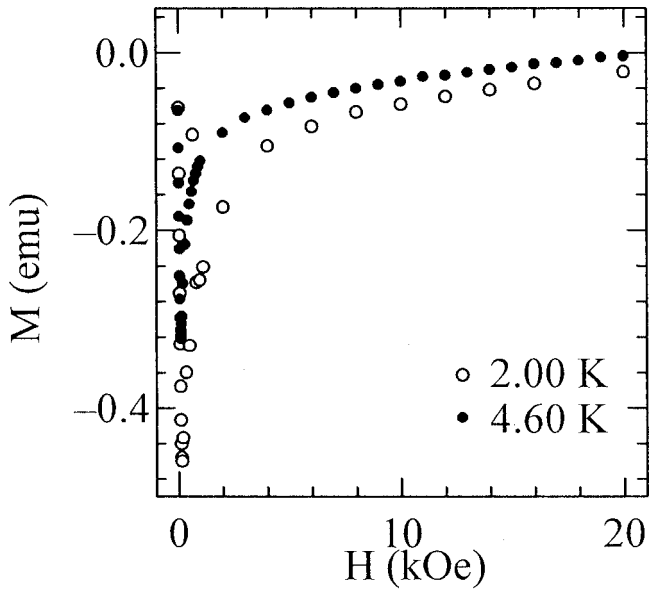

FIG. 6. Field dependence of the magnetization M in the superconducting state measured at 4.6 (●) and 2.0 K (○).

electronic state due to the lattice transformation at around 120 K. It has been reported that HfV_2 undergoes a cubic to orthorhombic structural transition at $T_L \sim 120$ K, which is accompanied by a volume increase and anomalous behavior of the resistivity, heat capacity, and susceptibility.[12,14] The increase in χ below 60 K corresponds to the decrease in K. Therefore, this increase in χ is not due to a paramagnetic impurity that has nothing to do with K in general.

χ and K are written as[15]

$$\chi = \chi_{3d}(T) + \chi_{3d\ {\rm orb}} + \tfrac{2}{3}\chi_{4s} + \chi_{\rm dia} + \chi_{5d}(T) + \chi_{5d\ {\rm orb}} + \tfrac{2}{3}\chi_{\rm Pauli}, \tag{1}$$

$$K = K_{3d}(T) + K_{3d\ {\rm orb}} + K_{4s} \tag{2}$$

with

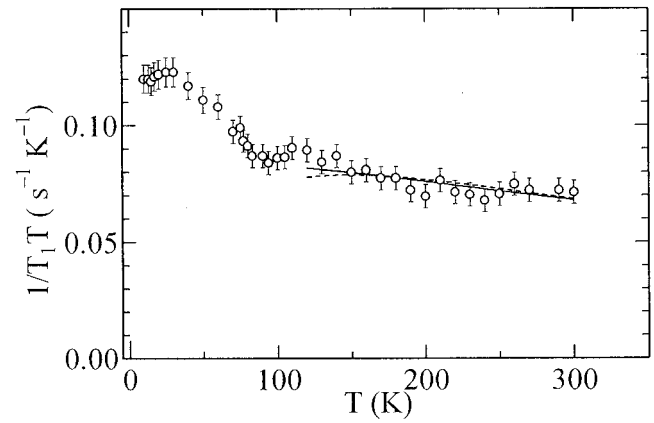

FIG. 7. Temperature dependence of ^{51}V spin-lattice relaxation rate $1/T_1T$ in the normal state reported in Ref. 6. Best fitting curves based on a *simple Lorentzian model* and a *two-peak model* are shown by solid and dotted curves, respectively.

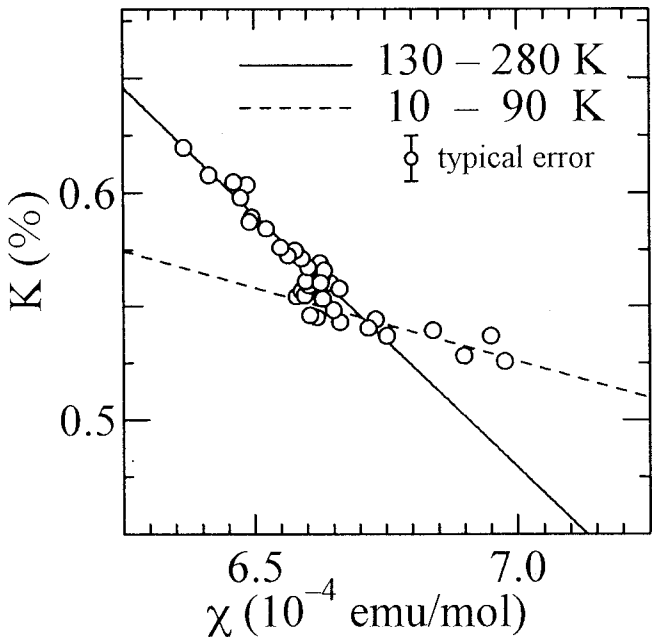

FIG. 8. K is plotted against χ with the temperature as an implicit parameter.

$$K_i = H_{\rm hf}^i \frac{\chi_i}{N_A \mu_B} \quad (i = 3d,\ 3d\ \text{orb},\ 4s), \tag{3}$$

where $\chi_{3d}(T)$, χ_{4s}, $\chi_{3d\ \rm orb}$, and $\chi_{\rm dia}$ are the spin susceptibilities due to V $3d$ and $4s$ electrons, the orbital susceptibility due to V $3d$ electrons and the diamagnetic susceptibility due to V and Hf core electrons, respectively. $\chi_{5d}(T)$ and $\chi_{5d\ \rm orb}$ are the spin susceptibility and the orbital susceptibility due to Hf $5d$ electrons, respectively. $\chi_{\rm Pauli}$ is the spin susceptibility due to V $3p$, Hf $5p$, Hf $6s$ and other electrons. $\chi_{\rm dia} \sim -4.6\times10^{-5}$ emu/mol is given by Gupta.[16] $K_{3d}(T)$, $K_{3d\ \rm orb}$, and K_{4s} arise in proportion to $\chi_{3d}(T)$, $\chi_{3d\ \rm orb}$, and χ_{4s}, respectively. $H_{\rm hf}^i$ represents the corresponding hyperfine field. N_A is the Avogadro's number. $H_{\rm hf}^{3d\ \rm orb} = 216$ kOe/μ_B is given from the formula, $H_{\rm hf}^{3d\ \rm orb} = 2\mu_B \langle r^{-3}\rangle \times 0.75$, and $\langle r^{-3}\rangle = 1.56\times10^{25}\,\rm cm^{-3}$ calculated for V atom with $[3d]^4$ configuration by Freeman and Watson.[17] We neglect the diamagnetic shift induced by the orbital current of V inner closed shells since it is generally an order of magnitude smaller. $\chi_{\rm dia}$ due to Hf core electrons, $\chi_{5d}(T)$, $\chi_{5d\ \rm orb}$, and $\chi_{\rm Pauli}$ do not contribute to K. We assume that $\chi_{5d}(T)$ is negligibly small because the density of states (DOS) due to Hf $5d$ electrons is only one-tenth of that of V $3d$ electrons according to a band calculation.[18]

K is plotted against χ with the temperature as an implicit parameter in Fig. 8. K has a linear relation with χ in both temperature ranges between 130 and 280 K (high-temperature region), and between 10 and 90 K (low-temperature region). The least-squares fit yields the relation, $K(\%) = 2.0 - 0.22\chi(10^{-4}\,\text{emu/mol})$ (solid line) in the high-temperature region, while $K(\%) = 0.98 - 0.065\chi(10^{-4}\,\text{emu/mol})$ (dotted line) in the low-temperature region. $H_{\rm hf}^{3d} = -250$ kOe/μ_B is obtained in the high-temperature region, while the hyperfine field is estimated to be -72 kOe/μ_B in the low-temperature region. -250 kOe/μ_B is somewhat large but appropriate to a hyperfine field of $3d$ transition elements, which means that the exchange interaction between core s and $3d$ electrons is strong. This result supports the assumption that $\chi_{5d}(T)$ is negligibly small is reasonable. The change to -72 kOe/μ_B is considered to be due to a change in the electronic states induced by lattice transformation at T_L. This change is too large to attribute to a change in the core-polarization due to V $3d$ spin. Since the magnitude of the hyperfine field due to the $4s$ Fermi contact interaction is one order larger than that due to the $3d$ core-polarization, a strong $4s$-$3d$ mixing sometimes reduces the magnitude of the hyperfine field of transition elements. Such $4s$-$3d$ mixing has been observed as $H_{\rm hf}^{3d} = -16$ kOe/μ_B for ^{61}Ni in the superconducting $LuNi_2B_2C$ (Ref. 19) and $H_{\rm hf}^{4d} = -27.5$ kOe/μ_B for ^{91}Zr in the weak ferromagnetic $ZrZn_2$ (Ref. 20). We consider the above reduced hyperfine field as the effect of $4s$-$3d$ mixing induced by the lattice transformation. The fraction of $N_{3d}(\varepsilon_F)$ that has $4s$ character is estimated to be about 16%.

B. A combined analysis of χ, K, and $1/T_1T$

In this section, we analyze the temperature dependence of χ and K together with that of $1/T_1T$, and discuss the change in the electronic state induced by the lattice transformation.

Since $K_{3d}(T)$ is expressed with $H_{\rm hf}^{3d}$ and the DOS of $3d$ electrons $N_{3d}(\varepsilon)$ in general, Eq. (2) becomes

$$K = \frac{2\mu_B H_{\rm hf}^{3d}}{N_A} \int_{-\infty}^{\infty} d\varepsilon \left(-\frac{\partial f}{\partial \varepsilon}\right) N_{3d}(\varepsilon - \mu) + K_{3d\ \rm orb} + K_{4s}, \tag{4}$$

where $f(\varepsilon)$ is the Fermi-Dirac distribution function.

$1/T_1T$ is written as

$$\frac{1}{T_1T} = \left(\frac{1}{T_1T}\right)_{3d\ \rm spin} + \left(\frac{1}{T_1T}\right)_{3d\ \rm orb} + \left(\frac{1}{T_1T}\right)_{4s}, \tag{5}$$

where $(1/T_1T)_{3d\ \rm spin}$, $(1/T_1T)_{3d\ \rm orb}$, and $(1/T_1T)_{4s}$ represent the contribution due to the $3d$ spin, $3d$ orbital angular momentum, and $4s$ spin, respectively. $(1/T_1T)_{3d\ \rm spin}$ and $(1/T_1T)_{3d\ \rm orb}$ depend on the symmetry of $3d$ orbitals, and are expressed by the factors q and p that are functions of the relative weight of $d\varepsilon$ and $d\gamma$ orbitals at the Fermi surface as follows.[21,22]

$$\left(\frac{1}{T_1T}\right)_{3d\ \rm spin} = \frac{4\pi k_B}{\hbar}\left(\frac{\gamma_n \hbar H_{\rm hf}^{3d}}{N_A}\right)^2 qK(\alpha) \times \int_{-\infty}^{\infty} d\varepsilon \left(-\frac{\partial f}{\partial \varepsilon}\right) N_{3d}^2(\varepsilon - \mu), \tag{6}$$

and

TABLE I. Relaxation rate and Knight shift.

	$(1/T_1T)_{3d}(0)$ ($s^{-1}K^{-1}$)	$(1/T_1T)_{4s}$	$K_{3d}(0)$	$K_{3d\ \mathrm{orb}}$ (%)	K_{4s}
Low temperature region	0.12	1.9×10^{-5}	−0.12	0.66	8.4×10^{-4}
High temperature region					
Simple Lorentzian model	0.061	0.022	−0.35	0.85	0.029
Two-peak model	0.013	0.016	−0.19	0.90	0.025

$$\left(\frac{1}{T_1T}\right)_{3d\ \mathrm{orb}}=\frac{4\pi k_B}{\hbar}\left(\frac{\gamma_n\hbar H_{\mathrm{hf}}^{3d\ \mathrm{orb}}}{N_A}\right)^2 p \times\int_{-\infty}^{\infty}d\varepsilon\left(-\frac{\partial f}{\partial\varepsilon}\right)N_{3d}^2(\varepsilon-\mu), \tag{7}$$

$K(\alpha)$ reflects the electron correlation.

If $N_{3d}(\varepsilon)$ has a sharp peak near the Fermi level, $(1/T_1T)_{3d\ \mathrm{spin}}$ and $(1/T_1T)_{3d\ \mathrm{orb}}$ depend on temperature in the same way. Therefore, we write

$$\left(\frac{1}{T_1T}\right)_{3d}=\left(\frac{1}{T_1T}\right)_{3d\ \mathrm{spin}}+\left(\frac{1}{T_1T}\right)_{3d\ \mathrm{orb}}. \tag{8}$$

The modified Korringa relation is obtained from Eqs. (4) and (6)–(8),

$$\left(\frac{1}{T_1T}\right)_{3d}=k(T)[K_{3d}(T)]^2, \tag{9}$$

$$k(T)=\frac{4\pi k_B}{\hbar}\left(\frac{\gamma_n}{\gamma_e}\right)^2\left[\frac{(H_{\mathrm{hf}}^{3d})^2qK(\alpha)+(H_{\mathrm{hf}}^{3d\ \mathrm{orb}})^2p}{(H_{\mathrm{hf}}^{3d})^2}\right] \times\frac{k_BT\int[N_{3d}(\varepsilon)]^2f(\varepsilon)[1-f(\varepsilon)]d\varepsilon}{(\int N_{3d}(\varepsilon)f(\varepsilon)[1-f(\varepsilon)]d\varepsilon)^2}. \tag{10}$$

The Korringa relation

$$\left(\frac{1}{T_1T}\right)_{4s}=\frac{4\pi k_B}{\hbar}\left(\frac{\gamma_n}{\gamma_e}\right)^2K_{4s}^2 \tag{11}$$

is assumed.

1. Low-temperature region (10≦T≦90 K)

At sufficiently low temperature $k(T)$ does not depend on temperature, being a constant k,

$$k=\frac{4\pi k_B}{\hbar}\left(\frac{\gamma_n}{\gamma_e}\right)^2\left[\frac{(H_{\mathrm{hf}}^{3d})^2qK(\alpha)+(H_{\mathrm{hf}}^{3d\ \mathrm{orb}})^2p}{(H_{\mathrm{hf}}^{3d})^2}\right]. \tag{12}$$

We obtain the following relation from Eqs. (2), (5), (8), (9), and (11),

$$\frac{1}{T_1T}=k[K-K_{3d\ \mathrm{orb}}-K_{4s}]^2+26.3K_{4s}^2. \tag{13}$$

We fit this equation to the observed data by the least-squares method, obtaining the best fitted parameters $k=9.4\,s^{-1}K^{-1}$, $K_{3d\ \mathrm{orb}}=0.66\%$, and $K_{4s}=8.4\times10^{-4}\%$. $\chi_{3d\ \mathrm{orb}}=3.4\times10^{-4}$ emu/mol is calculated from $K_{3d\ \mathrm{orb}}$. K_{4s} is found to be negligibly small. From $H_{\mathrm{hf}}^{4s}=1.12\times10^3$ kOe/μ_B (Ref. 21) and $\chi_{4s}=2\mu_B^2N_{4s}(\varepsilon_F)$, χ_{4s} and the DOS of $4s$ electrons $N_{4s}(\varepsilon_F)$ are estimated to be 8.4×10^{-8} emu/mol and 1.3×10^{-3} states $(\mathrm{eV})^{-1}$/V spin, respectively. $K(\%)=0.98-0.065\chi(10^{-4}\ \mathrm{emu/mol})$ is rewritten as

$$\chi(10^{-4}\ \mathrm{emu/mol})=-15[K(\%)-0.66]+3.4+1.5, \tag{14}$$

where K_{4s} and χ_{4s} are neglected, and $\chi_{\mathrm{dis}}+\chi_{5d\mathrm{orb}}+\frac{2}{3}\chi_{\mathrm{Pauli}}$ is found to be 1.5×10^{-4} emu/mol from Eq. (1). The temperature dependence of χ calculated according to Eq. (14) and the experimental data of K is shown in Fig. 3 by the closed circles.

We can estimate the total DOS of the conduction electrons $N(\varepsilon_F)$ from the electronic specific-heat coefficient $\gamma=2(1+\lambda)\pi^2k_B^2N(\varepsilon_F)/3$, where λ is the electron-phonon coupling constant. By using the values $\lambda=1.14$ and $\gamma=47.7\,\mathrm{mJ\,mol^{-1}\,K^{-2}}$,[6] $N(\varepsilon_F)=2.36$ states $(\mathrm{eV})^{-1}$/V spin is obtained. The total spin susceptibility is given by $2\mu_B^2N(\varepsilon_F)=3.1\times10^{-4}$ emu/mol at sufficiently low temperatures compared with (bandwidth)/k_B. This agrees well with $\chi-\chi_{3d\ \mathrm{orb}}=3.6\times10^{-4}$ emu/mol observed at 10 K. By subtracting $\chi_{\mathrm{dia}}+\chi_{5d\mathrm{orb}}+\frac{2}{3}\chi_{\mathrm{Pauli}}$, $\chi_{3d}(0)$ is estimated to be 2.1×10^{-4} emu/mol. The ratio of this value to the total spin susceptibility is the ratio of $N_{3d}(\varepsilon_F)$ to $N(\varepsilon_F)$. This ratio and $N_{3d}(\varepsilon_F)$ are estimated to be 0.68 and 1.60 states $(\mathrm{eV})^{-1}$/V spin, respectively. The obtained physical quantities are listed in Tables I and II.

2. High-temperature region (130≦T≦280 K)

We make an analysis based on a narrow-band model for $N_{3d}(\varepsilon)$ since the temperature dependence of $k(T)$ is important.

The temperature dependence of $K_{3d}(T)$ and $(1/T_1T)_{3d}$ is calculated from Eqs. (4), (6), and (7). The temperature-dependent chemical potential μ is determined by the relation

$$n=\int_{-\infty}^{\infty}d\varepsilon f(\varepsilon)N_{3d}(\varepsilon-\mu), \tag{15}$$

TABLE II. Density of states and magnetic susceptibility.

	$N(\varepsilon_F)$	$N_{3d}(\varepsilon_F)$	$N_{4s}(\varepsilon_F)$	$N_{3d}(\varepsilon_F)/N(\varepsilon_F)$	$\chi_{3d}(0)$	$\chi_{3d\ \mathrm{orb}}$	χ_{4s}	$\chi_{\mathrm{dia}}+\chi_{5d\ \mathrm{orb}}+\frac{2}{3}\chi_{\mathrm{Pauli}}$
	[states $(\mathrm{eV})^{-1}$/V spin]				(10^{-4} emu/mol)			
Low temperature region	2.36	1.60	1.3×10^{-3}	0.68	2.1	3.4	8.4×10^{-4}	1.5
High temperature region								
Simple Lorentzian model	<1.84[a]	1.22	4.5×10^{-2}	>0.66[a]	1.6	4.4	2.9×10^{-2}	0.80
Two-peak model	<0.89[a]	0.66	3.8×10^{-2}	>0.73[a]	0.85	4.7	2.5×10^{-2}	0.31
Band calculation[b]	0.91	0.64		0.70				

[a] $\chi_{\mathrm{dia}}+\chi_{5d\ \mathrm{orb}}>0$ is assumed though $\chi_{5d\ \mathrm{orb}}$ is not known.
[b] Reference 18.

where n is the number of $3d$ electrons. The following two models are assumed. *Simple Lorentzian model*

$$N_{3d}(\varepsilon)=\frac{N_A W}{\pi\{(\varepsilon-\varepsilon_0)^2+W^2\}}, \tag{16}$$

and *Two-peak model*

$$N_{3d}(\varepsilon)=\frac{3N_A}{2\pi(1+r)}\left[\frac{1}{W_1}\sqrt{\tfrac{4}{3}W_1^2-(\varepsilon+\varepsilon_1)^2}+\frac{r}{W_2}\sqrt{\tfrac{4}{3}W_2^2-(\varepsilon-\varepsilon_2)^2}\right], \tag{17}$$

where W, W_1, and W_2 are the bandwidths of respective $N_{3d}(\varepsilon)$ and ε_0, ε_1, and ε_2 are the energies of the peak position measured from the Fermi level. In the *two-peak model*, r is the ratio of the two parts of $N_{3d}(\varepsilon)$, which should be cut off for energy making the argument of the square root negative.

By substituting Eqs. (16) and (17) into Eqs. (4), (6), and (7), we fit the calculated K and $1/T_1T$ to the observed temperature dependence of them simultaneously by the least-squares method in order to determine $N_{3d}(\varepsilon_F)$, $K_{3d\ \mathrm{orb}}$, K_{4s}, and $(1/T_1T)_{4s}$.

a. DOS estimated by the *simple Lorentzian model*. The results of the best fittings of K and $1/T_1T$ with parameters, $W=500$ K and $\varepsilon_0/W=0.70$, are shown in Figs. 4 and 7 by the solid curves. The relation $qK(\alpha)+0.76p=0.019$ is obtained. The values $q=0.22$ and $p=0.18$ reported by Däumer, Khan, and Lüders[22] for $C15$ structures HfV_2H_x and $Hf_{0.5}Zr_{0.5}V_2H_x$ make $K(\alpha)$ negative, which do not seem reasonable. As $K(\alpha)\geqq 0$ p should be very small, less than 0.025. From the best fitted parameters and the equations discussed above various physical quantities are estimated and listed in Tables I and II.

b. DOS estimated by the *two-peak model*. The results of the best fittings of K and $1/T_1T$ with parameters, $W_1=500$ K, $W_2=160$ K, $\varepsilon_1/W_1=1.10$, $\varepsilon_2/W_2=1.15$, and $r=0.50$ are shown in Figs. 4 and 7 by dotted curves. $qK(\alpha)+0.76p=0.014$. Because $K(\alpha)\geqq 0$ p should be very small, less than 0.019. Various physical quantities estimated are summarized in Tables I and II.

Ormeci *et al.*[18] made the first-principles electronic structure calculations with a full-potential linear muffin-tin orbital method for $C15$ Laves phase compound HfV_2. They obtained $N_{3d}(\varepsilon_F)=140$ states/Ry per unit cell. By considering that eight HfV_2 formulas are contained in a unit cell, $N_{3d}(\varepsilon_F)$ is derived as 0.64 states $(\mathrm{eV})^{-1}$/V spin. They have shown that $N_{5d}(\varepsilon_F)$ is 14.5 states/Ry per unit cell, that the total contribution of V $3p$ and Hf $5p$ electrons is 27 states/Ry per unit cell, and that the contribution of $4s$ and $6s$ electrons is a few states/Ry per unit cell. $N_{3d}(\varepsilon_F)/N(\varepsilon_F)$ was calculated to be 0.70. This ratio is comparable with the values estimated from the above two models and our experimental results. Our above analysis that $N_{4s}(\varepsilon_F)$ is negligibly small is consistent with their result.

By considering that the temperature dependence of $1/T_1T$ between 20 and 100 K is explained by a narrow $N_{3d}(\varepsilon)$ with a bandwidth of about 100 K as discussed in the previous paper,[6] the present $W=500$ and $W_1=500$ K seem to reflect the change in the electronic state induced by the lattice transformation. $W_2=160$ K suggests that a part of a narrow band realized at low temperature still remains at high temperature. $\varepsilon_0/W=0.70$, $\varepsilon_1/W_1=1.10$, and $\varepsilon_2/W_2=1.15$ mean that the Fermi levels in both models are not on the peak of $N_{3d}(\varepsilon)$. This is consistent with the band calculation[18] in which the Fermi level crosses a relatively high local minimum of $N_{3d}(\varepsilon)$. It should be noted that $N_{4s}(\varepsilon_F)$ at high-temperature region is 32 times larger than that at low-temperature region.

V. KNIGHT SHIFT IN THE SUPERCONDUCTING STATE

The ^{51}V K measured at 12 MHz coincides with that at 6 MHz as shown in Fig. 5. This looks unreasonable because the magnitude of the magnetization M due to the Meissner effect at 6 MHz is larger than that at 12 MHz. Feyerherm *et al.*[23] reported an abnormal field dependence of K in the superconducting state for the HFS UPd_2Al_3, that is, the magnitude of the negative K at 5 kOe is smaller than that measured at 10 kOe. They ascribed this anomaly to the pair breaking due to the Pauli paramagnetic limiting effect. It is also reported[10,24] that the paramagnetic limiting effect on K and H_{c2} is observed in the same strong electron-phonon coupling superconductor V_3Si. The Pauli paramagnetic limiting

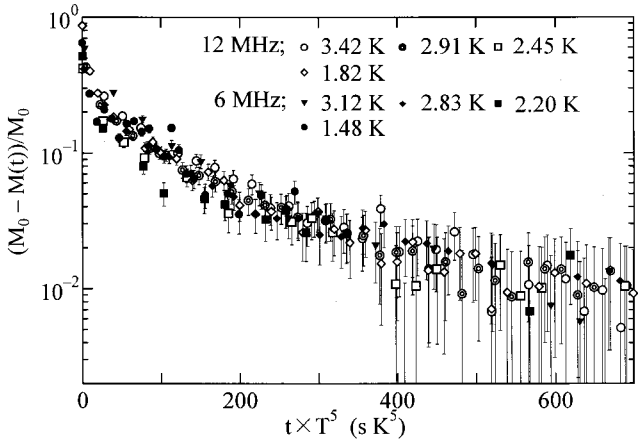

FIG. 9. The recovery $[M_0-M(t)]/M_0$ of the nuclear magnetization is plotted against $t\times T^5$.

effect on the behavior of K must exist in HfV_2. In our NMR measurement, the pair breaking due to magnetic field, which makes a positive contribution to χ, is larger at 12 MHz than at 6 MHz. Because the hyperfine field is negative, the Knight shift due to the pair breaking at 12 MHz is more negative than that at 6 MHz, which can explain the observed coincidence of K.

To estimate the temperature dependence of the intrinsic K and to discuss the symmetry of the order parameter, we must evaluate $K_{\rm dia}$ due to the Meissner effect. We use the formula given in Refs. 25–27,

$$K_{\rm dia}=-\frac{4\pi(1-N_x)|M|}{H}. \tag{18}$$

Our sample is a packed powder in a cylinder form with a diameter of 6 mm and a length of 5 mm. N_x is the demagnetization factor that is assumed to be 0.2 from the shape of the sample.[25,28] The filling factor of the sample is assumed to be 0.7. From the observed M in Fig. 6, we estimate $K_{\rm dia}=-0.03\%$ at 4.6 K, and $K_{\rm dia}=-0.05\%$ at 2.0 K for K measured at 12 MHz, and $K_{\rm dia}=-0.10\%$ at 4.6 K, and $K_{\rm dia}=-0.17\%$ at 2.0 K for K measured at 6 MHz. We have another formula,

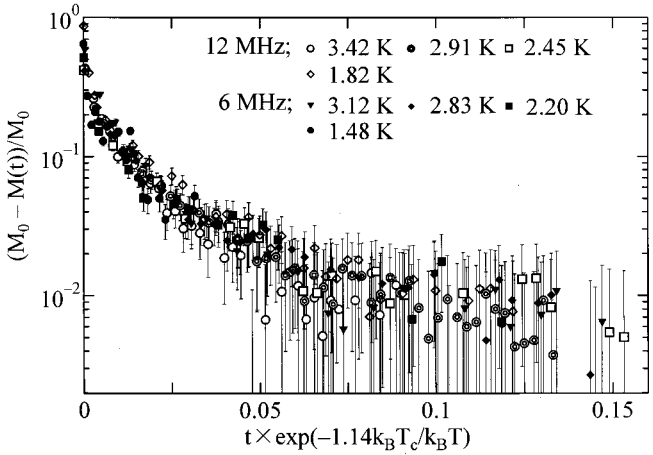

FIG. 10. $[M_0-M(t)]/M_0$ of the nuclear magnetization is plotted against $t\times\exp(-1.14k_BT_c/k_BT)$.

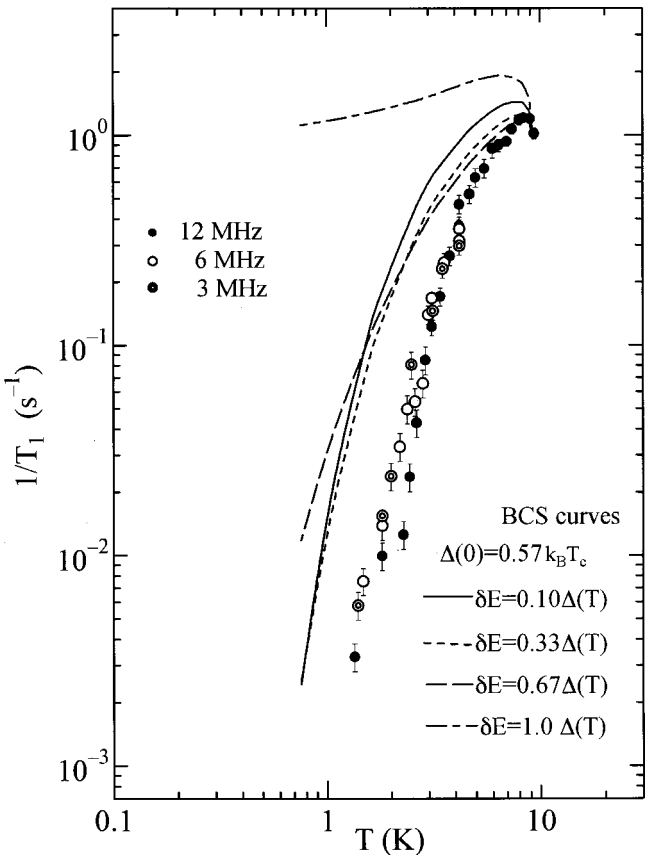

FIG. 11. ^{51}V $1/T_1$ in the superconducting state (Ref. 6). Curves show the calculated temperature dependence for BCS gap $\Delta(0)=0.57k_BT_c$ and various broadenings δE.

$$K_{\rm dia}=-\frac{H_{\rm cl}}{H}\frac{\ln(\beta e^{-0.5}d/\xi)}{\ln(\lambda/\xi)}, \tag{19}$$

where $H_{\rm cl}$ is the lower critical field, d the distance between vortices, ξ the coherence length, λ the penetration depth, and $\beta=0.381$ (Ref. 29). It should be noted that we have obtained larger values of $|K_{\rm dia}|$ when we used Eq. (19). We adopt the corrections based on Eq. (18) because Eq. (18) uses the experimental values of M while Eq. (19) is deduced theoretically. By subtracting $K_{\rm dia}$ from the raw K, the corrected values of K at 4.6 and 2.0 K are obtained and shown in Fig. 5. The broken curves in Fig. 5 illustrate the expected temperature dependence of the corrected K's. They do not agree with each other, owing to the Pauli paramagnetic limiting effect discussed above.

Here, we find the fact that the low-temperature limiting value of the corrected K is larger than $K_{3d\,\rm orb}=0.66\%$ estimated in Sec. IV B 1, indicating that the contribution of $3d$ spin to K vanishes completely well below T_c. This is interpreted as the loss of all of $3d$ spin susceptibility, that is, the Cooper pair is in a spin singlet state.

In the superconducting state, we have reported that $1/T_1$ shows a very small enhancement just below T_c and a T^5

dependence well below T_c, and that the electronic specific heat is proportional to T^3 at low temperatures.[6] We discussed this behavior in terms of a p wave ABM gap model in which the superconducting energy gap is anisotropic and vanishes at poles on the Fermi surface.

To reconfirm the T^5 dependence of $1/T_1$, we plot the recovery $[M_0-M(t)]/M_0$ of nuclear magnetization measured at various low temperatures against $t\times T^5$ in Fig. 9, where $M(t)$ is the nuclear magnetization observed at time t after a saturation pulse and M_0 is that at $t=\infty$. The data points fall into a band. $[M_0-M(t)]/M_0$ measured at various temperatures scales to $t\times T^5$ within experimental errors. We try to plot the same recovery against $t\times\exp(-2\Delta/k_BT)$ in Fig. 10. The data points also fall into a band. However, we have to choose a small energy gap $2\Delta/k_BT_C=1.14$ in Fig. 10, which is too small in order to represent a BCS gap. Moreover, this very small energy gap cannot explain the whole temperature dependence of $1/T_1$ in the superconducting state with any broadening δE as shown in Fig. 11. Thus it is impossible to explain the temperature dependence of the recovery of the nuclear magnetization by BCS gap. We can conclude that $1/T_1$ has the T^5 dependence well below T_c. Therefore, the energy gap vanishes at points on the Fermi surface (ABM gap), and the Cooper pair is not of s wave but d wave.

Indeed, a d-wave ABM gap is derived from an even-parity $d\gamma$ wave.

$$\frac{(\cos k_x+\cos k_y-2\cos k_z)}{\sqrt{6}}\pm i\frac{(\cos k_x-\cos k_y)}{\sqrt{2}}, \quad (20)$$

or an even-parity $d\varepsilon$ wave

$$\sin(k_x)\sin(k_y)+\varepsilon\sin(k_y)\sin(k_z)+\varepsilon^2\sin(k_z)\sin(k_x), \quad (21)$$

pairing in the relative coordinate. Where $\varepsilon=(-1+i\sqrt{3})/2$. There are nodes in the [1,1,1] and equivalent directions on the Fermi surface both in $d\gamma$ and $d\varepsilon$ states. The Cooper pair in HfV_2 is considered to be of spin singlet $d\gamma$ or $d\varepsilon$ wave, for example.

VI. CONCLUSION

The Knight shift K of ^{51}V and the magnetic susceptibility χ have been measured to investigate the change in the electronic state due to the lattice transformation and the symmetry of the superconducting order parameter in HfV_2.

In the normal state, K has a linear relation with χ in the temperature ranges both between 130 and 280 K, and between 10 and 90 K, and the hyperfine field in each temperature range is obtained as -250 and $-72\,\mathrm{kOe}/\mu_B$, respectively. This reduction in the magnitude of hyperfine field is considered to be due to a s-d mixing induced by the martensitic lattice transformation. In the high-temperature region, we can explain the temperature dependence of K and $1/T_1T$ based on the narrow $3d$ band model. $N_{3d}(\varepsilon_F)/N(\varepsilon_F)$ obtained from K and $1/T_1T$ agrees with that estimated from the band calculation. $N_{4s}(\varepsilon_F)$ is found to be negligibly small in both temperature ranges.

Well below T_c, the Knight shift due to $3d$ spin vanishes completely. This means that the Cooper pair is of spin singlet. By considering that the T^5 dependence of $1/T_1$ and the T^3 dependence of specific heat are explained with the anisotropic energy gap that has nodes on the Fermi surface, the Cooper pair is considered to be of ABM $d\gamma$ or $d\varepsilon$ wave, for example.

ACKNOWLEDGMENTS

The authors are sincerely grateful to Profs. K. Asayama and K. Mizuno for valuable discussions. They also wish to thank Prof. K. Miyake for detailed discussions on the ABM gap states. This work is partially supported by the Grant-in-Aid for Scientific Research from the Ministry of Education, Japan.

[1] T. Matsuura and K. Miyake, J. Phys. Soc. Jpn. **55**, 29 (1986); **55**, 610 (1986).
[2] P. W. Anderson and C. C. Yu, *Highlights of Condensed Matter Theory*, edited by F. Bassani, F. Fumi, and M. P. Tosi (North-Holland, Amsterdam, 1985), p. 767.
[3] H. Kusunose and K. Miyake, J. Phys. Soc. Jpn. **65**, 3032 (1996).
[4] K. Vladar and A. Zawadowsky, Phys. Rev. B **28**, 1564 (1983); **28**, 1582 (1983); **28**, 1596 (1983).
[5] B. Lüthi, M. Herrmann, W. Assmus, H. Schmidt, H. Rietschel, H. Wühl, U. Gottwick, G. Sparn, and F. Steglich, Z. Phys. B: Condens. Matter **60**, 387 (1985).
[6] Y. Kishimoto, N. Shibata, T. Ohno, Y. Kitaoka, K. Asayama, K. Amaya and T. Kanashiro, J. Phys. Soc. Jpn. **61**, 696 (1992).
[7] P. W. Anderson and W. F. Brinkman, *The Physics of Liquid and Solid Helium*, edited by K. H. Benneman and J. B. Koterson (Wiley, New York, 1979), Vol. 2, p. 177.
[8] P. W. Anderson and P. Morel, Phys. Rev. **123**, 1911 (1961).
[9] M. J. Parsons, P. J. Broun, J. Crangle, K-U. Neumann, B. Ouladdiaf, T. J. Smith, N. K. Zayer, and K. R. A. Ziebeck, J. Phys.: Condens. Matter **10**, 8523 (1998).
[10] Y. Kishimoto, T. Ohno, and T. Kanashiro, J. Phys. Soc. Jpn. **64**, 1275 (1995).
[11] S. V. Vonsovsky, Yu. A. Izumov, and E. Z. Kurmaev, *Superconductivity of Transition Metals* (Springer-Verlag, Berlin, 1982), p. 375.
[12] A. C. Lawson and W. H. Zachariasen, Phys. Lett. **38A**, 1 (1972).
[13] General Catalog, Kojundo Chemical Laboratory Co. Ltd. (2000).
[14] J. H. Hafstrom, G. S. Knapp, and A. T. Aldred, Phys. Rev. B **17**, 2892 (1978).
[15] A. M. Clogston, A. G. Gossard, V. Jaccarino, and Y. Yafet, Phys. Rev. Lett. **9**, 262 (1962).
[16] R. R. Gupta, in *Diamagnetic Susceptibility*, edited by O. Madelung, Landolt-Börnstein, New Series, Group II, Vol. 16 (Springer-Verlag, Berlin, Heidelberg, 1986), p. 402.
[17] A. J. Freeman and R. E. Watson, *Magnetism II A*, edited by G. T. Rado and H. Suhl (Academic, New York, 1965), p. 165.

[18] A. Ormeci, F. Chu, J. M. Wills, T. E. Mitchel, R. C. Albers, D. J. Thoma, and S. P. Chen, Phys. Rev. B **54**, 12 753 (1996).
[19] K. Ikushima, H. Yasuoka, A. Ohno, H. Takagi, R. J. Cava, J. J. Krajewski, and W. F. Peck, Jr., J. Phys. Soc. Jpn. **66**, 1130 (1997).
[20] M. Kontani, T. Hioki, and Y. Masuda, J. Phys. Soc. Jpn. **39**, 665 (1975).
[21] Y. Yafet and V. Jaccarino, Phys. Rev. **133A**, 1630 (1964).
[22] W. Däumer, H. R. Khan, and K. Lüders, Phys. Rev. B **38**, 4427 (1988).
[23] R. Feyerherm, A. Amato, F. N. Gygax, A. Schenck, C. Geibel, F. Steglich, N. Sato, and T. Komatsubara, Phys. Rev. Lett. **73**, 1849 (1994).
[24] T. P. Orlando, E. J. McNiff Jr., S. Foner, and M. R. Beasley, Phys. Rev. B **19**, 4545 (1979).
[25] T. Ohno, Y. Kishimoto, K. Miyatani, and M. Ishikawa, Physica C **250**, 227 (1995).
[26] K. Mizuno, A. Mahajan, H. Alloul, and T. Saito (unpublished).
[27] M. Takigawa, P. C. Hammel, R. H. Heffner, and Z. Fisk, Phys. Rev. B **39**, 7371 (1989).
[28] D. Rossier and D. E. MacLaughlin, Phys. Kondens. Mater. **11**, 66 (1970).
[29] P. G. de Gennes, *Superconductivity of Metals and Alloys* (Benjamin, New York, 1966).